6.4

AIRBORNE DOPPLER RADAR OBSERVATIONS OF TURBULENCE IN MARINE STRATOCUMULUS

Marie Lothon*(1), Donald H. Lenschow(1), Dave Leon(2) and Gabor Vali(2)

(1) National Center for Atmospheric Research, Boulder, CO
(2) Department of Atmospheric Science, University of Wyoming, Laramie, WY

1. INTRODUCTION

Because of its large global coverage and the net cloud radiative forcing associated with it, the stratocumulus-topped boundary layer (STBL) is an important component of the climate system. In summer 2001, the DYCOMS-II field experiment (the second DYnamics and Chemistry Of Marine Stratocumulus field experiment) was aimed at probing the persistent STBL off the coast of southern California in order to better understand their physics and dynamics (Stevens et al, 2002). Entrainment of dry overlying air into the relatively cool and moist atmospheric boundary layer and drizzle are two important processes that remain poorly understood and quantified. Atmospheric turbulence plays a crucial role in both processes.

Doppler velocity measurements made by the Wyoming Cloud Radar (WCR) mounted on the NCAR C-130 during this experiment gave us an opportunity to complement the in situ observations of turbulence, since the radar can provide data from the full depth of the boundary layer simultaneously. While the aircraft was flying 60 km diameter quasi-Lagrangian circles at different levels in the STBL and in the overlying free troposphere, the 95 GHz (3 mm wavelength) WCR observed the cloudy atmosphere below with two downward-looking beams. One of the antennas looked straight down and the other looked backward (32.5° from the vertical). The radar used a 250 ns pulse with 1.6 kW peak power and 0.7° beamwidth. The mean Doppler velocity was estimated using pulse pair processing. Previously, the radar had been mounted on the Wyoming University King Air aircraft and proved very useful for observing finescale stratocumulus structure (Vali et al., 1998).

The high frequency of the measurements of the Doppler velocity along the two beams of the Wyoming Cloud Radar allowed a study of the finescale structure of the Doppler velocity field, using the structure function and the autocorrelation function. Like the Fourier spectrum, these functions can be used to calculate parameters which characterize the turbulence— e.g. eddy lengthscale or dissipation—but unlike it, they can conveniently be calculated from an irregular sampling of velocities.

*corresponding author address: Marie Lothon, National Center for Atmospheric Research, P. O. Box 3000, Boulder, CO 80307-3000; *email*: lothon@ucar.edu

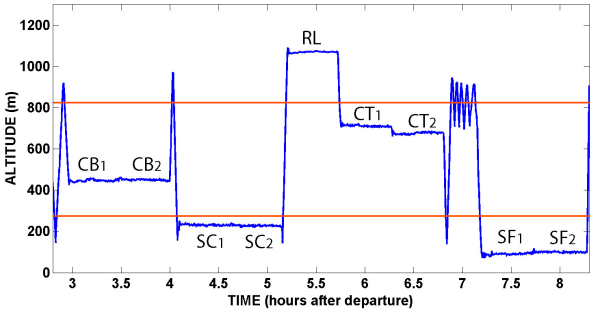

Figure 1: *Time series of the altitude flown by the C-130 during RF07. Each named leg is a circle of about 60 km diameter.*

Here we present the turbulent characteristics that were deduced from the WCR Doppler velocities observed during one nocturnal flight (RF07). This flight had the most uniform distribution of drizzle among the nine DYCOMS flights (Van Zanten et al., 2004). For the use of the Doppler velocities, we mainly focus here on the radar leg (RL, see Fig 1), which was flown at an altitude of 1070 m, about 200 m above the cloud top (825 m), that is high enough to probe the entire boundary layer. The cloud base was about 275 m. Eight legs probed the STBL, two at each of the four levels flown (Fig 1): near cloud top (CT1 and CT2), just above cloud base (CB1 and CB2), between cloud base and the surface (SC1 and SC2) and 95 m above the surface (SF1 and SF2). The in situ measurments made during these eight legs were used for comparison with the radar measurements.

2. DATA PROCESSING

In order to obtain the turbulent component of the Doppler velocity on each beam along the circle legs, a preliminary mean analysis was conducted. The geometry of the airborne trajectory allowed us to use a method analogous to the VAD (Velocity Azimuth Display) to get the mean wind components on the beams and deduce the turbulent component on each beam, after correcting for aircraft motion. This method has been named the

AVAD (Airborne Velocity Azimuth Display) technique by Leon and Vali (1997). 2.5 minute segments ($\sim$ 15 km) of the residual component were detrended to get the turbulent component. The in situ air velocity measurements were also partitioned into 2.5 minute segments for the legs flown within the boundary layer. The circular flight path makes the longitudinal (u_x) and lateral (v_y) components vary sinusoidally. This sinusoidal signal due to the mean wind was removed from each segment to get the turbulent components. The in situ vertical velocity (w) was simply detrended over each segment.

3. TURBULENCE ANALYSIS METHODOLOGY

The structure function and the autocorrelation function of the fluctuations of a wind component allow us to describe the fine-scale turbulence (see Monin and Yaglom (1971) for the general definition of structure function and more details. For a turbulent component u_i', the second-order structure function is:

$$D_{ii}(\mathbf{r}) = \overline{[u_i'(\mathbf{x}+\mathbf{r}) - u_i'(\mathbf{x})]^2} \tag{1}$$

where **x** denotes the position vector and **r** the displacement vector. Similarly, the autocorrelation function of this component is:

$$R_{ii}(\mathbf{r}) = \overline{u_i'(\mathbf{x})u_i'(\mathbf{x}+\mathbf{r})}. \tag{2}$$

Note that $R_{ii}(0)$ is equal to the variance of u_i'. These two functions are commonly used to get the characteristics of the turbulence, like dissipation of turbulent kinetic energy or lengthscales.

If the field is locally isotropic, and in the inertial subrange, $D_{ii}(\mathbf{r})$ is proportional to the lateral structure function $D_{NN}(\mathbf{r})$, which is obtained when u_i is perpendicular to **r** and follows a 2/3 power law in the inertial subrange:

$$D_{NN} \cong \frac{4}{3} \times 4A\varepsilon^{2/3} r^{2/3}. \tag{3}$$

ε denotes the dissipation that characterizes the inertial subrange and A is the spectral constant, which we take equal to 0.52 (Fairall and Larsen, 1986). The structure functions that we can calculate with the Doppler velocity measurements during DYCOMS, are the lateral structure function D_{NN}—using the vertical beam— and $D_{\alpha\alpha}$— using the oblique beam, where α is the angle between **r** and the direction of the beam. Taking into account the geometry and the properties of the structure function in the inertial subrange and in case of local isotropy:

$$D_{\alpha\alpha} = \frac{3}{4}(1 + \frac{1}{3}\sin^2\alpha) D_{NN}. \tag{4}$$

The integral scale of a variable, which is a measure of the length over which a variable is relatively well correlated with itself, can be deduced from the autocorrelation function:

$$L_{ii} = \int_0^\infty \frac{R_{ii}(r)}{R_{ii}(0)} dr \tag{5}$$

A good estimate of the integral scale is obtained by taking the maximum of (Lenschow and Stankov, 1986):

$$F_{ii}(r) = \int_0^r \frac{R_{ii}(r_1)}{R_{ii}(0)} dr_1. \tag{6}$$

That is

$$L_{ii} = \max\{F_{ii}(r)\}_r. \tag{7}$$

Thus, calculating R_{NN} and $R_{\alpha\alpha}$ from the WCR Doppler measurements allows us to estimate L_{NN} and $L_{\alpha\alpha}$.

D_{NN}, $D_{\alpha\alpha}$, R_{NN} and $R_{\alpha\alpha}$ were calculated for each 2.5 minute segments at each range and with r ranging from 5 to 1000 m, every 5 m, from the Doppler velocity fluctuations measurements along the two down-looking beams. We neglected the change due to the trajectory curvature ($\sim$30°) over the domain of variation of r. For a given range, an average over the 12 segments lead to a mean structure function and a mean autocorrelation function that were used to obtain profiles of the integral scales and dissipation within the STBL. The averaged autocorrelation functions of all ranges were used to obtain the vertical profile of the horizontal integral scales for each measured component. The averaged structure functions calculated from the radar Doppler velocity measurements were fit to a modeled structure function described in the next section, which assumes a von Kármán energy spectrum, using the measured integral scales and taking into account the radar pulse volume averaging, as well as a white noise contribution.

A similar averaging process was followed for the in situ air velocity measurements within the STBL to allow a comparison with the radar measurements. The autocorrelation functions and spectra were calculated for every segment and averaged over each circle. Integral scales of w and $u_\alpha = w\cos\alpha + u_x \sin\alpha$ were obtained from the autocorrelation functions, and turbulent dissipation from v_y spectra, chosen as the most reliable spectra. w had an inertial subrange with a somewhat steeper slope which made the estimates of the dissipation less accurate. u_x spectrum showed some noise at high frequency and its energy seemed overestimated in the inertail subrange, relative to w and v_y spectra. It turned out to be due to an inaccuracy on the sensitivity coefficent of the true airspeed.

4. EFFECT OF THE WCR PULSE VOLUME ON THE TURBULENCE SPECTRUM

The radar measurement is not a point measurement but results from an average within the volume defined by

the pulse length and the beam width. We looked at the effect of this averaging on the turbulence functions. For that, we considered an idealized spectrum and studied the effect of the velocity averaging within the radar pulse volume, taking account of the characteristics of the WCR beam and of the measured integral scales. The effect on structure functions was then deduced from the Fourier transform of the filtered spectra.

The method is discussed by Srivastava and Atlas (1974). The assumptions made are: (1) Taylor's hypothesis is fulfilled; (2) The reflectivity is uniform inside the radar pulse volume; (3) The beam illumination function within the pulse volume depends only on the distance from the considered point to the center of the volume; (4) The beam width of the radar is small enough to neglect the divergence of the radial velocity within the volume; (5) Turbulence is homogeneous and isotropic. Hypotheses (2) and (3) imply that the mean of the Doppler spectrum is an average of the point radial velocities weighted by the mean illumination function and that

$$\bar{v}(\mathbf{R}) = \int_V v(\mathbf{R}_1) I(\mathbf{R} - \mathbf{R}_1) d\mathbf{R}_1, \qquad (8)$$

where the integration is made over the pulse volume. The Fourier transform of eq. (8) changes the convolution into a product of spectral density and the beam illumination function (or beam filter function). Considering k_1 in the beam direction, hypothesis (4) states that the velocity spectral function is equal to ϕ_{11}. Denoting the beam filter function ϕ_I and the wave vector **k**, the longitudinal and transverse one-dimensional spectra can be written

$$S_L(k_1) = \int \phi_{11}(\mathbf{k}) \phi_I(\mathbf{k}) dk_2 dk_3 \qquad (9)$$

$$S_N(k_2) = \int \phi_{11}(\mathbf{k}) \phi_I(\mathbf{k}) dk_1 dk_3. \qquad (10)$$

Here, $S_L(k_1)$ would be obtained if the radar beam were parallel to the flight direction (forward-looking beam), and $S_N(k_2)$ is the spectrum for the downward-looking beam, which is orthogonal to the flight direction.

The beam filter function depends on the characteristics of the beam which we approximated by:

$$\phi_I(k) = \left(\frac{\sin(k_1 c/2)}{(k_1 c/2)} \right)^2 \cdot \exp^{(-\mu_2^2 k_2^2)} \cdot \exp^{(-\mu_3^2 k_3^2)} \qquad (11)$$

where c is half the pulse length and $\mu_2 = \mu_3 = 0.3003\, R\theta$, for range R and beamwidth $\theta = 0.7°$. For homogeneous and isotropic turbulence (hypothesis 5):

$$\phi_{11} = \left(1 - \frac{k_1^2}{k^2} \right) \frac{E(k)}{4\pi k^2} \qquad (12)$$

where $k^2 = k_1^2 + k_2^2 + k_3^2$. We assumed a von Kármán energy spectrum:

$$E(k) = \alpha_{3D} \varepsilon^{3/2} L^{5/3} \frac{(Lk)^4}{(1 + (Lk)^2)^{17/6}} \qquad (13)$$

where $\alpha_{3D} \approx 1.6$ and $L = 2.68\, L_{NN}$. This means that we also assumed that the integral scales are long relative to the size of the radar pulse volume, and that the volume averaging has a negligible effect on the integral scale estimate.

From the von Kármán energy spectrum, the idealized longitudinal and transverse spectra were calculated numerically. The corresponding longitudinal and transverse autocorrelation functions or structure functions were then deduced using the Fourier transform of the longitudinal and transverse spectra. The modeled trailing structure function was deduced using equation (4) and the measured trailing integral scale.

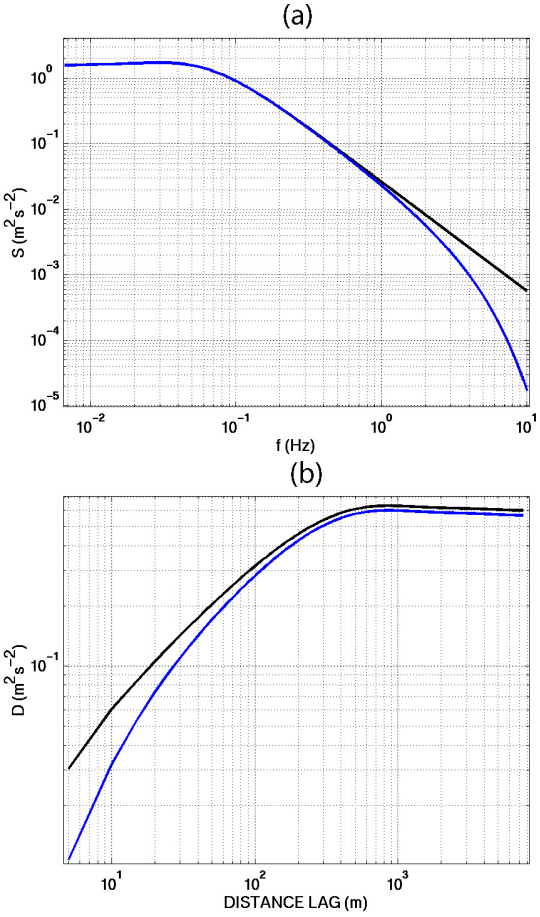

Figure 2: *Effect of the velocity averaging within the radar pulse volume at an altitude of 405 m, (a) on the transverse spectrum and (b) on the structure function, at an altitude In both figures, the black line displays the case of no volume averaging (F_N) and the blue line the case of averaging (S_N).*

Figure 2 shows the effect of the volume averaging on the ideal transversal spectrum and structure function at an altitude of 405 m. At this altitude, the observed integral scale for the nadir Doppler velocity is $L_{NN} = 145$ m and the range of R =645 m corresponds to a beamwidth

of $R\theta$ =8 m. This figure shows the decrease of energy for scales close to or smaller than the pulse length. It shows as well that the volume averaging effect is spread over all scales of the structure function. The measured structure functions do not show the strong drop for small lags, likely because of noise that has the opposite effect of the volume averaging.

With no volume averaging, the von Kármán one-point double-sided transverse spectrum can be calculated analytically:

$$F_N(k,R) = \frac{3}{110}\alpha\varepsilon.^{2/3}\frac{3L(R)^{-2}+8k^2}{(L(R)^{-2}+k^2)^{11/6}}, \qquad (14)$$

which leads to the variance

$$\sigma(R)^2 = \frac{15}{110}\sqrt{\pi}\frac{\Gamma(1/3)}{\Gamma(11/6)}(\varepsilon(R)L(R))^{2/3}. \qquad (15)$$

This true variance and a noise level added to the volume-effect corrected von Kármán structure function are the two parameters that were used to fit the observed structure functions with the modeled ones at each range, using the observed integral scales and the characteristics of the beam at the same range. Equation (15) is then used to deduce the dissipation from the true variance obtained from the fit.

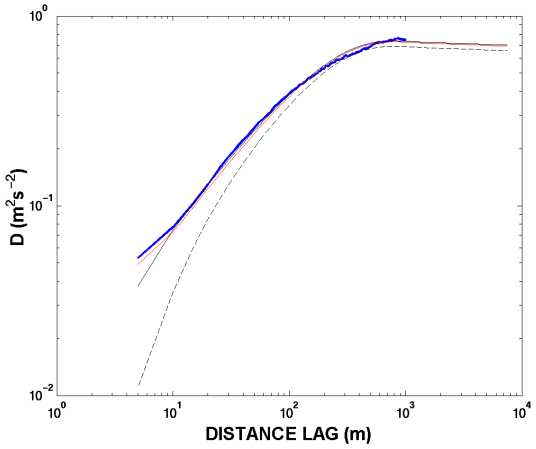

Figure 3: *Blue solid line: Observed structure function of the nadir Doppler velocity at 240 m. Red line: best fit with the model of a Von Kármán energy spectrum, taking account of the volume averaging and of a certain amount of noise that is given by the fit along with the true variance. Black solid line: Corresponding ideal Von Kármán structure function. Black dashed line: Structure function after applying the volume averaging on the ideal Von Kármán structure function.*

Figure 3 shows an example of a mean structure function observed at 240 m altitude on the nadir beam and the modeled structure function that leads to the best fit. The structure function corresponding to the ideal original von Kármán spectrum is also shown, along with the structure function resulting from only the volume averaging. As stated previously, both the true variance and the level of uncorrelated noise were determined by best fits to the observations. For the example of Fig. 3, the variance was found to be 0.35 m^2s^{-2} and the noise 0.04 m^2s^{-2}.

5. RESULTS

5.1 Integral scales

Figures 4 displays the mean profiles of the integral scales of the Doppler velocities measured on both beams for flight RF07. The errorbars represent the variation of integral scale deduced from the segments separately along the circle. These profiles agree well with the horizontal integral scales calculated with the in situ velocity measurements, which means that it is possible to get this important turbulent lengthscale from Doppler radar measurements in cloudy air. Figure 4 shows the effect of the strong inversion at the top of the boundary layer: the vertical eddies are compressed and thus the integral scale decreases. Similarly, it decreases near the surface. This is typical of "squashed" turbulence (Kristensen et al., 1983). Unlike the integral scale of the vertical velocity, the integral scale of the trailing Doppler velocity, because of the contribution from the horizontal component, increases at the top and at the bottom of the boundary layer due to the widening of the horizontal eddies close to these interfaces. The difference between the two profiles also shows that the turbulence is far from isotropic for scales larger than 200 m, especially near the interfaces.

5.2 Turbulent energy

Vali et al. (1998) observed previously in marine stratocumulus that the fluctuations of the Doppler velocity were smaller than the actual fluctuations of the air velocity measured in situ. The contrary was observed in clear air. The difference is due to the different scatterers, which are hydrometeors in the first case and insects in the second case. During flight RF07 of DYCOMS, we found a rather large departure between the variance of the Doppler velocity along the vertical beam and the variance of the vertical velocity measured by the in situ gust probe. Figure 5 shows the profiles of both the variance of the Doppler velocity during the radar leg, taking account of the noise level and the volume averaging as explained previously, and the variance of the vertical velocity measured by the in situ gust probe during the legs flown within the STBL. We expect the Doppler velocity variance to be smaller than the air velocity variance, because of the velocity averaging, but this effect should increase from the cloud top down to the surface. This effect was actually

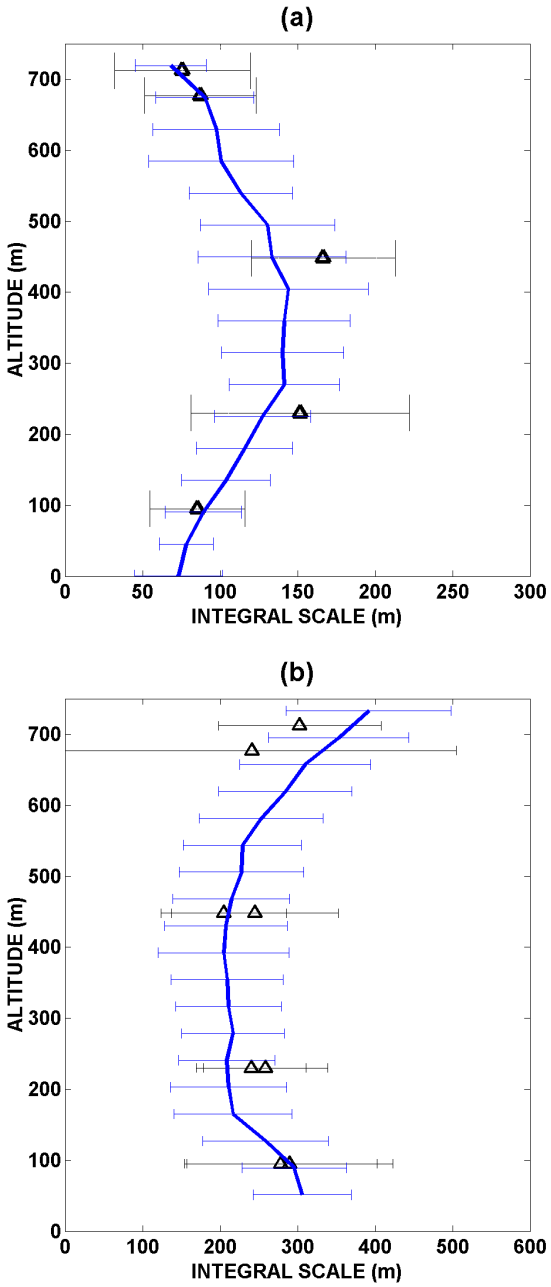

Figure 4: *Solid line: mean integral scales calculated from the nadir radial velocities (a) and from the trailing radial velocities (b), for flight RF07. The triangles represent the mean integral scale of the vertical velocity from the in situ measurements.*

responsible for less than 10% decrease of the variance and compensated by the noise which was around 0.05 m^2s^{-2}. Thus it could not explain the large departure that we observe in the upper part of the STBL. The most probable explanation seems to be a correlation between the updrafts and drizzle.

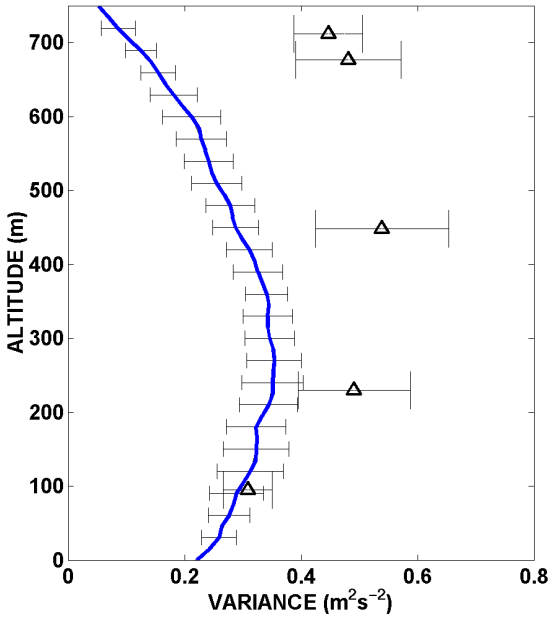

Figure 5: *Solid line: Vertical profile of the observed variance of the nadir Doppler velocity. Triangles: Vertical profile of the variance of the in situ vertical gust component.*

We found evidence of this correlation by conditionally sampling the in situ gust probe and microphysics probe measurements. We obtained droplet spectra from the 10 Hz measurements of the FSSP-100 and the 260X probes averaged over one circle leg conditioned by, respectively, positive and negative vertical velocity of the air. Figure 6 shows the two spectra that we observe just below cloud top. Drizzle drops, which are most responsible for the radar signal, are in significantly larger numbers in updrafts. The two spectra lead to a fall velocity difference up to 0.4 ms^{-1}. This feature was also found at cloud base. But below cloud the effect was considerably smaller and was not seen or even reversed close to the surface. This decreasing correlation between updrafts and drizzle was also observed by Vali et al. (1998). Figure 6 demonstrates qualitatively that the link between the cloud drops and the vertical motion of the air does significantly influence the Doppler velocity, and is consistent with the increasing departure with altitude that we can see on Fig. 5. However, it remains difficult to estimate quantitatively this correlation, because of the sampling

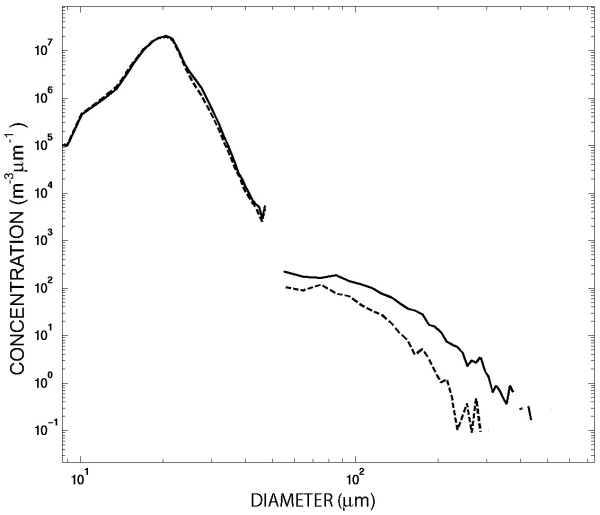

Figure 6: *Averaged size distribution during CT1, in two bins of conditional sampling over the air vertical velocity. The first bin (dashed line) is made with -3 $ms^{-1} \leq w \leq$-0.5 ms^{-1} The second bin (solid line) is made with 0.5 $ms^{-1} \leq w \leq$3 ms^{-1}*

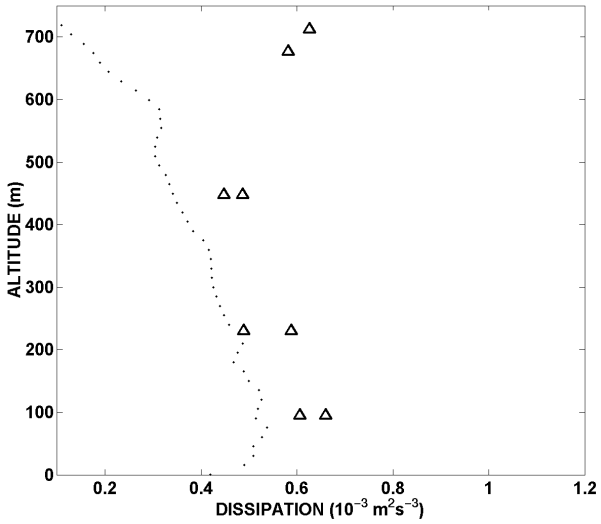

Figure 7: *Mean profile of the dissipation calculated from the radar measurements and in situ measurements. The in situ dissipation estimates (triangles) are deduced from the in situ lateral wind component. The dots represent the estimates from radar measurements.*

issues imbedded in the measurements of the rare large drizzle drops (see P1.5 extended abstract). According to this latter study and the estimates found for the fluctuations of the Doppler velocity due to the drop fall velocity ($\sim$ 0.01 m^2s^{-2}), the correlation between the vertical velocity of the air and the fall velocity would need to be greater than 0.8 to explain such a departure. Because of the uncertainty due to the sparsity of the large drops, these estimates of the fall velocity fluctuations might be underestimated. But such a large correlation does seem plausible.

5.3 Turbulence dissipation

Figure 7 displays the mean profile of the dissipation, found with both the radar (nadir) and the in situ measurements. Both measurements were again over 2.5 minute segments. The dissipation estimates from in situ measurements were calculated using the spectrum of the lateral horizontal wind component in the aircraft coordinates. The inertial subrange was fitted with the theoretical -5/3 power law to get the dissipation estimate. The mean dissipation is obtained from a mean spectrum over each circle flown within the STBL. The estimates from the radar measurements shown in Fig. 7 are calculated from equation (15) using the true variance found with the best fit of the observed structure function with the modeled one. These estimates showed a strong sensitivity to the noise level. As previously observed on other vertical profiles and consistently with Fig. 5, the largest departure is found near cloud top. But the agreement is better lower in the cloud. The best agreement is found around 250 m, where the best fit could be made with the von Kármán model. It is also an altitude high enough from the surface and low enough for the correlation between the air velocity and the fall velocity to be small. These profiles show that the dissipation remains difficult to estimate with a cloud radar. As well, the weak dissipation that is expected in marine stratocumulus makes the task more difficult.

6. CONCLUSIONS

The exceptionnal data set of DYCOMS-II experiment and the combination it made of in situ aircraft measurements and Doppler measurements with the high resolution 95 GHz Wyoming Cloud Radar drove us to attempt to use the radar measurements to get the turbulence characteristics in marine stratocumulus cloud. In particular, the most uniform and one of the deepest cloud was studied for this purpose. Taking account of the velocity averaging due to the radar pulse volume, the structure function and autocorrelation function of the fluctuations of the wind component along the radar beams were used to get the integral scales, the variance and the dissipation rates. This work showed that it is actually possible to get the integral scales from Doppler radar measurements in cloudy atmosphere, thus allowing the observation of this essential turbulent parameter within the whole cloud layer probed by the radar. A strong correlation between updrafts and drizzle drops prevented us from retrieving ac-

curately the turbulent dissipation, but the observation of this large correlation is an important result for the understanding of the marine stratocumulus processes.

Acknowledgements

Support for the DYCOMS-II project was provided by NSF Grant ATM-0097053 and ATM-0094956. NSF and ONR provided major funding for the acquisition, development and research use of the Wyoming Cloud Radar. This work was made possible thanks to ASP, MMM and ATD divisions of NCAR, the University of Wyoming and the Ministry of Foreign Affairs of France that provided a BFE Lavoisier grant to the first author during a postdoctoral fellowship.

REFERENCES

Fairall, C. W. and S. E. Larsen, 1986: Inertial dissipation methods and turbulent fluxes at the air-ocean interface, *Boundary-Layer Meteorol.*, **34**, 287–301.

Kristensen, L., P. Kirkegaard, and D. H. Lenschow, 1983: *Squashed atmospheric turbulence*, Denmark. Riso National Lab., Roskilde, Riso-R-478, Jan., 79 pp.

Lenschow, D. H. and B. B. Stankov, 1986: Length scales in the convective boundary layer, *J. Atmos. Sci.*, **43**, 1198–1209.

Leon, D. and G. Vali, 1997: Retrieval of three-dimensional particle velocity from airborne doppler radar data, *J. Atmos. Oceanic Technol.*, **15**, 860–870.

Monin, A. S. and A. M. Yaglom, 1971: *Statistical fluid mechanics: mechanics of turbulence*, John L. Lumley.

Srivastava, R. C. and D. Atlas, 1974: Effect of finite radar pulse volume on turbulence measurements, *J. Appl. Meteorol.*, **13**, 472–480.

Stevens, B. et al, 2002: Dynamics and Chemistry of Marine Stratocumulus – DYCOMS-II, *Bull. Am. Meteorol. Soc.*, **84**, 579–593.

Vali, G., R. Kelly, J. French, S. Haimov, D. Leon, R. McIntosh, and A. Pazmany, 1998: Finescale structure and microphysics of coastal stratus, *J. Atmos. Sci.*, **55**, 3540–3564.

Van Zanten, M. C., B. Stevens, G. Vali, and D. H. Lenschow, 2004: On drizzle rates in nocturnal marine stratocumulus, *Accepted at J. Atmos. Sci.*